Periodic travelling waves for a fourth order nonlinear evolution equation

Periodic travelling waves for a fourth order nonlinear evolution equation

Renato Colucci

Abstract. In this article we provide a travelling wave analysis for a fourth order non linear evolution equation. In particular we prove the existence of periodic travelling waves while we exclude the existence of solitary waves for proper values of the parameters. Moreover, we analyse the set of stationary solutions and provide a new proof of the existence of limit cycle for a related equation, that is, the Van der Pol equation.

Mathematics Subject Classification (2010). Primary 35B36; Secondary 35C07, 35Q86.

Keywords. Pattern formation, traveling wave solutions, fast and slow dynamics.

1. Introduction

In this article we consider the following fourth order nonlinear evolution equation

$$\begin{cases} u_t = \varepsilon u_{xxxx} + \nu u_{xxx} + [W'_\eta(u_x)]_x, & x \in I, \quad t > 0, \\ u(x,0) = u_0(x), & x \in I, \end{cases} \tag{1.1}$$

where

$$W_\eta(p) = \frac{1}{4\eta}(\eta p^2 - 1)^2,$$

$\varepsilon, \eta, \nu \in \mathbb{R}$ are positive parameters and I is a bounded interval. Equation (1.1) arises in pattern formation (see [6] and references cited therein) and due to its complexity has a mathematical interest by itself.
In [6] the case $\nu = 0$ has been considered, in particular the set of stationary solutions and the travelling waves have been analysed.
For $\nu = 0$ system (1.1) does not admit solitary waves solutions, the solutions describing travelling waves show an oscillatory behaviour at first stage of the dynamics and then blow up at infinite time. We will prove, using tools from singular perturbation theory, in section 3 below, that the presence of the term νu_{xxx} regularizes the oscillations and gives rise to a periodic travelling wave. It is worth noting that the problem of the existence of periodic travelling

waves has attracted interest of the researches in the last decades (see for instance [4] or [5]) due to their importance in describing spatio-temporal oscillations in natural phenomena such as epidemics ([15]) population dynamics ([2],[3]), fluid dynamics [14] etc...
Since in ou arguments we make use of the Van der Pol equation, in section 4 we provide a different proof of the existence of limit cycle using a new (according to our knowledge of the literature) positively invariant set. Finally, in section 5 we discuss what is the influence of the term νu_{xxx} to the set of stationary solutions and prove that they are divided into three classes with peculiar behaviour for large values of the spatial variable x. We end the article with some conclusive remarks in section 6.

2. Travelling waves

In this section we start the analysis of travelling waves for the problem (1.1). In order to do that we consider the usual ansatz, that is, we look for solution of the form

$$v(\xi) := u(x - ct).$$

Then, substituting in (1.1) we obtain

$$-cv' + \varepsilon v^{iv} + \nu v^{iii} + [W'_\eta(v')]' = 0, \tag{2.1}$$

and after integration it results

$$-cv + \varepsilon v^{iii} + \nu v^{ii} + [W'_\eta(v')] + K = 0, \tag{2.2}$$

where K is a real constant that we set equal to zero without loss of generality. We introduce the following energy that will be useful for the analysis of the previous equation:

$$E(t) = \frac{1}{2}\varepsilon v''^2 + W_\eta(v') - W_\eta(0) - cvv'. \tag{2.3}$$

Its derivative along the solution of (2.2) is:

$$E'(\xi) = -[\nu v''^2 + cv'^2]. \tag{2.4}$$

Inspired by (2.4), we consider two distinct cases that we analyse separately in the following sections.

2.1. Case $c > 0$.

In the case in which the parameters ν and c have the same sign we obtain analogous results as in [6]. By the use of Monotonicity of the Energy $E(t)$ it is possible to prove the following results:

Theorem 2.1. *For $c, \nu > 0$ the equation* (1.1) *does not admit solitary wave solutions.*

Theorem 2.2. *For $c, \nu > 0$ the system* (2.2) *does not admit periodic solutions.*

Remark 2.3. *Even if we are considering only the case $\nu > 0$ it is worth nothing that the same monotonicity arguments work also in the case $\nu, c < 0$.*

We end this subsection by analysing bounded solutions of equation (2.2). For simplicity we consider only the case $\nu, c > 0$. The corresponding system of ODE's obtained using the usual change of variable $u = u$, $u' = v$ and $v^{'} = w$ is

$$\begin{cases} u' = v, \\ v' = w, \\ \varepsilon w' = cu - v(\eta v^2 - 1) - \nu w. \end{cases} \tag{2.5}$$

The system admits one fixed point $O = (0, 0, 0)$, the Jacobian matrix at O is

$$J_O = \begin{pmatrix} 0 & 1 & 0 \\ 0 & 0 & 1 \\ \frac{c}{\varepsilon} & \frac{1}{\varepsilon} & -\frac{\nu}{\varepsilon} \end{pmatrix}, \tag{2.6}$$

while its trace and determinant are

$$trJ_O = -\frac{\nu}{\varepsilon} < 0, \qquad detJ_O = \frac{c}{\varepsilon} > 0.$$

In the following lines we compute the characteristic polynomial of J_0 together with its first and second derivatives

$$\begin{aligned} P(\lambda) &= \lambda^3 + \frac{\nu}{\varepsilon}\lambda^2 - \frac{1}{\varepsilon}\lambda - \frac{c}{\varepsilon}, \\ P'(\lambda) &= 3\lambda^2 + 2\frac{\nu}{\varepsilon}\lambda - \frac{1}{\varepsilon}, \\ P''(\lambda) &= 6\lambda + 2\frac{\nu}{\varepsilon}. \end{aligned}$$

Since $P(0) = -c < 0$ we always have at least one positive real eigenvalue. First of all we observe that the first derivative changes sign, then the polynomial results to be increasing outside the interval $(\frac{-\nu-\sqrt{\nu^2+3\varepsilon}}{3\varepsilon}, \frac{-\nu+\sqrt{\nu^2+3\varepsilon}}{3\varepsilon})$. Thus, if the eigenvalues are all real, one is positive and two are negative.
In the case of two complex conjugate eigenvalues λ_C, $\bar{\lambda_C}$ and one positive real eigenvalue λ_R we have, from the first order coefficient of the characteristic polynomial, that

$$|\lambda_C|^2 + 2\lambda_R \Re(\lambda_C) = -\frac{1}{\varepsilon},$$

from which we must have $\Re(\lambda_C) < 0$.
The above computation shows that we only have two cases:

(A) three real eigenvalues, one positive and two negative;
(B) one real positive eigenvalue and two complex conjugate eigenvalues with negative real parts.

In order to find the bifurcation value of the parameter c for passing from case (A) to case (B) we observe that what distinguishes the two cases is the sign of $P(\lambda)$ at its local maximum that it is attained at

$$\lambda_M = \frac{-\nu - \sqrt{\nu^2 + 3\varepsilon}}{3\varepsilon} = \frac{1}{\nu - \sqrt{\nu^2 + 3\varepsilon}}.$$

The value of the characteristic polynomial at λ_M is:

$$P(\lambda_M) = \frac{1}{\varepsilon}\left\{-c - \frac{\nu^2 + 2\varepsilon - \nu\sqrt{\nu^2+3\varepsilon}}{(\nu - \sqrt{\nu^2+3\varepsilon})^3}\right\} := \frac{1}{\varepsilon}(-c + c_1^*).$$

Then for $c \leq c_1^*$ we are in case (A) otherwise in case (B).
In order to study bounded solutions we can prove as in [6] the following result:

Lemma 2.4. *$E(\xi)$ is unbounded if and only if $u(\xi)$ is unbounded.*

It is clear that on bounded solutions the energy $E(\xi)$ is bounded and this happens if and only if

$$\lim_{\xi\to\pm\infty} E'(\xi) = 0,$$

that is, if and only if

$$\lim_{\xi\to\pm\infty} u'(\xi) = \lim_{\xi\to\pm\infty} u''(\xi) = 0.$$

Since $u \equiv 0$ is the unique constant solution we obtain the following result:

Theorem 2.5. *Let $c, \nu > 0$. All bounded solutions for $\xi > 0$ of equation* (2.2) *satisfy*

$$\lim_{\xi\to+\infty} u(\xi) = 0.$$

From the above analysis we conclude that the set of bounded solutions for $\xi > 0$ consists of solutions converging to the point O on its stable manifold.

2.2. Case $c < 0$.

We pass to consider the case in which the two parameters have opposite sign, for simplicity we set

$$\nu > 0, \quad \tilde{c} := -c > 0.$$

The equation reeds

$$\varepsilon u^{iii} + \nu u^{ii} + [W_\eta'(u')] + \tilde{c}u = 0, \tag{2.7}$$

while the energy and its derivative become:

$$\tilde{E}(t) = \frac{1}{2}\varepsilon u''^2 + W_\eta(u') - W_\eta(0) + \tilde{c}uu',$$
$$\tilde{E}'(t) = \tilde{c}u'^2 - \nu u''^2.$$

By a similar analysis of the previous section we obtain that for the characteristic polynomial of the Jacobian matrix at O we have only two cases:

(A) three real eigenvalues, one negative and two positive;
(B) one real negative eigenvalue and two complex conjugate eigenvalues with positive real parts.

In order to find the bifurcation value of the parameter $\tilde{c}$ we observe that what distinguishes case (A) from case (B) is the sign of $P(\lambda)$ at its local minimum that it is attained at

$$\lambda_m = \frac{-\nu + \sqrt{\nu^2+3\varepsilon}}{3\varepsilon} = \frac{1}{\nu + \sqrt{\nu^2+3\varepsilon}}.$$

The value at λ_m of the characteristic polynomial is:

$$P(\lambda_m) = \frac{1}{\varepsilon}\left\{\tilde{c} - \frac{\nu^2 + 2\varepsilon + \nu\sqrt{\nu^2+3\varepsilon}}{(\nu+\sqrt{\nu^2+3\varepsilon})^3}\right\} := \frac{1}{\varepsilon}(\tilde{c} - c_2^*).$$

Then for $c \leq c_2^*$ we are in case (A) otherwise in case (B).
Since the expression of $\frac{d}{d\xi}E(\xi)$ admits change of sign we expect that in this case ($c < 0$) a more interesting behaviour occurs with respect to that of the case $c > 0$. In particular we may conjecture the existence of homoclinic orbits (solitary waves) and of non trivial bounded solutions. The analysis of such problems will be addressed in the next sections.

3. Singular perturbation setting

We reconsider equation (2.7) in the context of fast-slow systems (see [13]) in order to use a perturbative approach to study its solutions.
We believe it is useful to adopt the standard notation which is common in the study of such kinds of problems. We consider the following change of variables:

$$x = w, \quad y_1 = v, \quad y_2 = u,$$

from which we obtain:

$$\begin{cases} \varepsilon\dot{x} = -\nu x - \tilde{c}y_2 - F_\eta(y_1) := f(x, y_1, y_2), \\ \dot{y_1} = x := g_1(x, y_1, y_2), \\ \dot{y_2} = y_1 := g_2(x, y_1, y_2), \end{cases} \tag{3.1}$$

where the parameter $0 < \varepsilon << 1$ is small, $x \in \mathbb{R}$ is called fast variable while $y = (y_1, y_2) \in \mathbb{R}^2$ are the slow variables, and

$$F_\eta(y_1) := y_1(\eta y_1^2 - 1).$$

Moreover, $\dot{x} = \frac{dx}{d\tau}$ where τ is called slow time. The previous system can be rewritten with respect to the so called fast time $t = \frac{\tau}{\varepsilon}$ obtaining:

$$\begin{cases} x' = -\nu x - \tilde{c}y_2 - F_\eta(y_1), \\ y_1' = \varepsilon x, \\ y_2' = \varepsilon y_1, \end{cases} \tag{3.2}$$

where $x' = \frac{dx}{dt}$. Systems (3.2)-(3.1) give rise to two singular systems, obtained by setting $\varepsilon = 0$, called slow and fast subsystem respectively:

$$\begin{cases} 0 = -\nu x - \tilde{c}y_2 - F_\eta(y_1), \\ \dot{y_1} = x, \\ \dot{y_2} = y_1, \end{cases} \tag{3.3}$$

$$\begin{cases} x' = -\nu x - \tilde{c}y_2 - F_\eta(y_1), \\ y_1' = 0, \\ y_2' = 0. \end{cases} \tag{3.4}$$

The above sub systems in many cases serve as a guide for the possible behaviour of the full system. Another important element in the singular perturbation theory consists in the following set

$$C_0 = \{(x, y) \in \mathbb{R}^3 : \quad f(x, y) = -\nu x - \tilde{c} y_2 - F_\eta(y_1) = 0\}, \tag{3.5}$$

which is called *Critical Manifold*. The idea is that, near the set C_0, solutions of the full system should behave like that of the slow subsystem on the set C_0.
In our case, since

$$D_x f(p), \qquad p \in C_0,$$

has no zero eigenvalues the critical manifold is called *Normally Hyperbolic*. Moreover, since

$$D_x f = -\nu < 0,$$

we obtain that the critical manifold C_0 is of *Attractive Type*.
For the sake of clarity we present the main result in the context of fast-slow system, that is, Fenichel's Theorem (see [13] Chapter 3, Theorem 3.1.4):

Theorem 3.1. *Suppose S_0 is a compact normally hyperbolic submanifold of the critical Manifold C_0 of the system*

$$\begin{cases} \varepsilon \dot{x} = f(x, y, \varepsilon), \\ \dot{y} = g(x, y, \varepsilon), \end{cases}$$

where $f : \mathbb{R}^m \times \mathbb{R}^n \times \mathbb{R} \to \mathbb{R}^m, g : \mathbb{R}^m \times \mathbb{R}^n \times \mathbb{R} \to \mathbb{R}^n$ are of class C^r $(r > 0)$ and $0 < \varepsilon << 1$. Then, for ε sufficiently small, the following hold:

1. *there exists a locally invariant manifold S_ε diffeomorphic to S_0. Local invariance means that trajectories can enter or live S_ε only trough its boundaries.*
2. *S_ε has Hausdorff distance $O(\varepsilon)$ (as $\varepsilon \to 0$) from S_0.*
3. *The flow on S_ε converges to the slow flow as $\varepsilon \to 0$.*
4. *S_ε is of class C^r.*
5. *S_ε is Normally Hyperbolic and has the same stability properties with respect to the fast variables as S_0 (attracting, repelling or of saddle type).*
6. *S_ε is usually not unique. In regions that remain at a fixed distance from ∂S_ε, all manifold satisfying (1)-(5) lie at a Hausdorff distance $O(e^{-\frac{K}{\varepsilon}})$ from each other for some $K > 0$, $K = O(1)$.*

The same conclusions as for S_0 hold locally for its stable and unstable manifolds:

$$W^s_{loc}(S_0) = \cup_{p \in S_0} W^s_{loc}(p), \qquad W^u_{loc}(S_0) = \cup_{p \in S_0} W^u_{loc}(p),$$

where we view points $p \in S_0$ as equilibria of the fast subsystem. These manifolds also persist for $\varepsilon > 0$ sufficiently small: there exist local stable and unstable manifolds $W^s_{loc}(S_\varepsilon)$ and $W^u_{loc}(S_\varepsilon)$, respectively, for which conclusions (1)-(6) hold if we replace S_ε and S_0 by $W^s_{loc}(S_\varepsilon)$ and $W^s_{loc}(S_0)$ (or similarly by $W^s_{loc}(S_\varepsilon)$ and $W^s_{loc}(S_0)$).

In order to have an hint of the possible behaviour of the system (3.1) we pass to the study of the two subsystems. In the context of fast-flow systems, the strategy consists in constructing a *candidate orbit* which is a concatenation of portions of trajectories belonging to the fast and slow subsystem. The idea is that, for ε sufficiently small, we expect that a true orbit of the full systems exists and it is close the candidate orbit.

From the above reasons we start by studying the slow subsystem which consists of differential-algebraic equation (DAE). The idea (see [13]) is to differentiate the system (3.3) till we find a complete differential system for the three variables. Differentiating (3.3) we obtain

$$\begin{cases} 0 = -\nu\dot{x} - \tilde{c}\dot{y}_2 - F'_\eta(y_1)\dot{y}_1, \\ \ddot{y}_1 = \dot{x}, \\ \ddot{y}_2 = \dot{y}_1, \end{cases}$$

and using (3.3) we can write a complete system

$$\begin{cases} \dot{x} = -\frac{\tilde{c}}{\nu}y_1 - \frac{1}{\nu}F'_\eta(y_1)x, \\ \dot{y}_1 = x, \\ \dot{y}_2 = y_1, \end{cases} \tag{3.6}$$

which describes the dynamics on C_0. We observe that the first two equations are independent of y_2 and then it is possible to study a two dimensional system. If we rewrite the system as a second order ODE we obtain the famous Van der Pol equation (see [9])

$$\ddot{y}_1 + \frac{1}{\nu}(3\eta y_1^2 - 1)\dot{y}_1 + y_1 = 0. \tag{3.7}$$

As a consequence the dynamics on C_0 is completely determined: there is one repulsive fixed point, that is O, surrounded by a limit cycle γ_0 which attracts all the solutions (see figure 1).

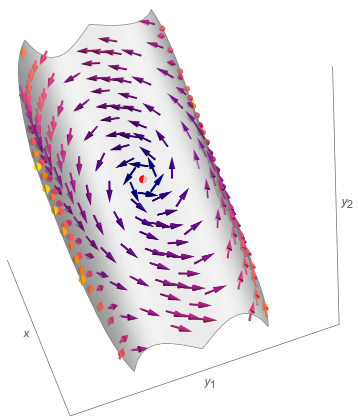

FIGURE 1. The slow flow on the critical Manifold C_0.

For the fast sub-system we observe that y_1 and y_2 are constant and play the role of parameters. For any fixed value of these parameters, say (y_{10}, y_{20}), we obtain the following asymptotic behaviour:

$$\lim_{t \to +\tau} x(\tau) = -\frac{\tilde{c}}{\nu} y_{20} - \frac{1}{\nu} F_\eta(y_{10}) := x_\infty.$$

We observe that $(x_\infty, y_{10}, y_{20})$ is a point of the Critical Manifold C_0.
The analysis of the two sub systems suggests that in a first stage of the dynamics (fast time τ) solutions approach the Slow Manifold S_ε and then slowly exhibit periodic behaviour.
The following result prove this conjecture.

Theorem 3.2. *For ε sufficiently small, system* (3.2) *admits a periodic orbit γ_ε which locally attracts nearby solutions.*

Proof. We have observed that the reduced system admits an attractive periodic orbit which is isolated. Moreover the Critical Manifold satisfies

$$D_x f(p) = -\nu < 0, \qquad \forall p \in C_0.$$

We define the following compact submanifold of C_0:

$$S_0 := C_0 \cap B_R(O),$$

where $B_R(O)$ is the closed ball of $\mathbb{R}^3$ with centre O and radius $R > 0$ to be chosen sufficiently large.
Then we can apply a result by Anosov (see Theorem 8.3 in [7] or its less general version contained in [8]). From Anosov's Theorem we obtain the existence of a periodic solution γ_ε with period T_ε such that

$$\gamma_\varepsilon \to \gamma_0, \quad T_\varepsilon \to T_0, \quad \text{as } \varepsilon \to 0,$$

where γ_0 is the limit cycle of the Slow Flow on C_0 with period T_0.
By Fenichel's Theorem (Theorem 3.1 item 5.) we have that both S_ε and S_0 share the same stability properties and since the dynamics on S_ε is approximated by that on S_0 (Theorem 3.1 item 3.) we conclude that the periodic orbit γ_ε locally attracts nearby solutions. □

While the rigorous results are valid only for $0 < \varepsilon << 1$, we observe that numerical simulations (see figure 2 below) suggest that periodic orbits persist also for higher values of ε, that is $\varepsilon \geq 1$. Moreover, the attraction appears to be global and this leads us to presume that the periodic orbit is a global attractor. These conjectures will be analysed in a future work.

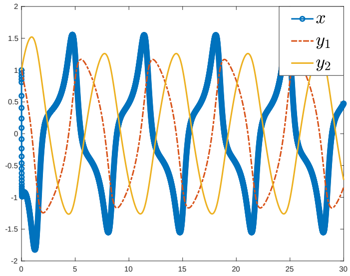

(A) $\varepsilon = 0.01$.

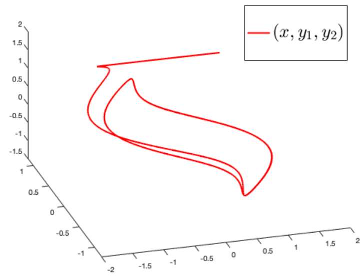

(B) $\varepsilon = 0.01$.

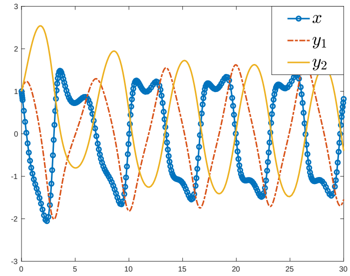

(C) $\varepsilon = 1$.

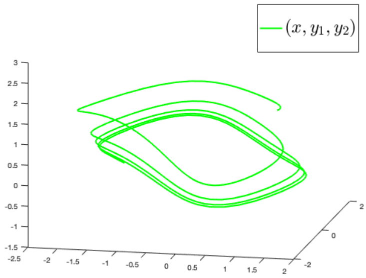

(D) $\varepsilon = 1$.

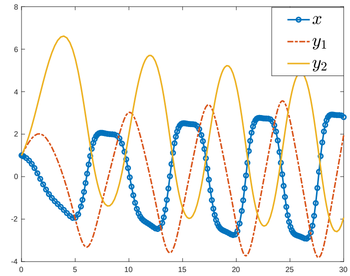

(E) $\varepsilon = 10$.

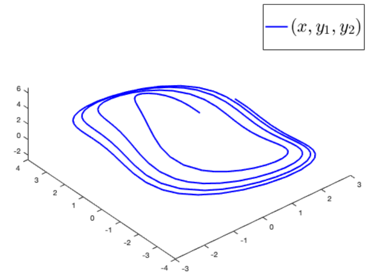

(F) $\varepsilon = 10$.

FIGURE 2. The time series and three dimensional graph of the periodic solution of system (3.1) for $\nu = \eta = \tilde{c} = 1$ and for ε as indicated, with $(x(0), y_1(0), y_2(0)) = (1, 1, 1)$. Panels (A) and (B) illustrate the theoretical results that are valid for $0 < \varepsilon << 1$. In particular, in panel (B) we are able to observe the initial fast dynamics which consists in rapidly approaching the limit cycle. In the remaining panels we explore the case $\varepsilon \geq 1$ which is outside the range of validity of rigorous results. Oscillations persist for $\varepsilon \geq 1$ without loosing stability, we do not observe initial fast dynamics but only a slow convergence to the periodic orbit (panels (D) and (F)).

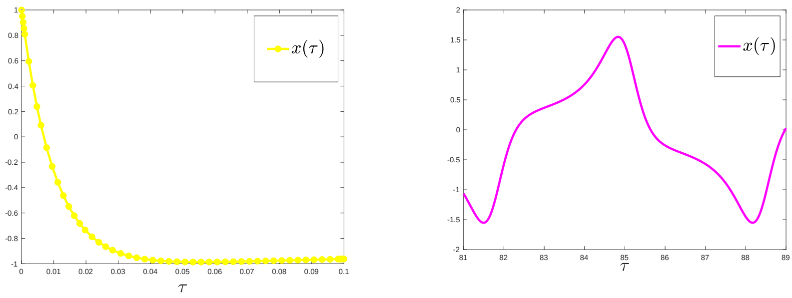

(A) (B)

FIGURE 3. In this figure we consider the case $\varepsilon = 0.01$, $\nu = \eta = \tilde{c} = 1$ and $(x(0), y_1(0), y_2(0)) = (1, 1, 1)$. The time interval in which fast dynamics occurs appears to be of order $O(\varepsilon)$ (panel(A)) while the period of oscillations is approximately $T \approx 7 \approx O(\varepsilon^{-\frac{1}{2}})$ showing a slow dynamics character (panel (B)).

3.1. Computation of the Slow Manifold

We recall that the critical manifold is given by

$$C_0 := \left\{ (x,y) \in \mathbb{R}^3 : \quad x = h_0(y_1,y_2) := -\frac{\tilde{c}}{\nu} y_2 - \frac{1}{\nu} F_\eta(y_1) \right\}.$$

In this section we derive an asymptotic expansion of the Slow manifold S_ε with respect to ε till order $O(\varepsilon^2)$ in the following form:

$$h_\varepsilon(y_1,y_2) = h_0(y_1,y_2) + \varepsilon h_1(y_1,y_2) + \varepsilon^2 h_2(y_1,y_2) + o(\varepsilon^2), \quad \text{as} \quad \varepsilon \to 0. \tag{3.8}$$

We differentiate with respect to t the equation $x = h_\varepsilon(y_1,y_2)$ from which we obtain:

$$x' = \frac{\partial h_\varepsilon}{\partial y_1} y_1' + \frac{\partial h_\varepsilon}{\partial y_2} y_2'.$$

Then using (3.2) we obtain the so called *Invariance Equation*:

$$f(h_\varepsilon(y_1,y_2), y_1, y_2) - \varepsilon \nabla h_\varepsilon(y_1,y_2) \cdot (g_1(x,y_1,y_2), g_2(x,y_1,y_2)) = 0, \tag{3.9}$$

that is

$$-\nu \left[h_\varepsilon(y_1,y_2) - h_0(y_1,y_2) \right] - \varepsilon \left[\frac{\partial h_\varepsilon}{\partial y_1} h_\varepsilon(y_1,y_2) + \frac{\partial h_\varepsilon}{\partial y_2} y_1 \right] = 0.$$

Using the Taylor expansion (3.8) we can write:

$$\begin{aligned} -\nu \left[h_1 + \varepsilon h_2 + o(\varepsilon) \right] = & \left[\left(\frac{\partial h_0}{\partial y_1} + \varepsilon \frac{\partial h_1}{\partial y_1} + o(\varepsilon) \right) (h_0 + \varepsilon h_1 + o(\varepsilon)) \right. \\ & \left. + \left(\frac{\partial h_0}{\partial y_2} + \varepsilon \frac{\partial h_1}{\partial y_2} + o(\varepsilon) \right) y_1 \right]. \end{aligned}$$

Collecting terms of order $O(1)$ we obtain:

$$-\nu h_1 = h_0 \frac{\partial h_0}{\partial y_1} + y_1 \frac{\partial h_0}{\partial y_2},$$

where

$$\frac{\partial}{\partial y_1} h_0 = -\frac{1}{\nu} F_\eta'(y_1), \qquad \frac{\partial}{\partial y_2} h_0 = -\frac{\tilde{c}}{\nu},$$

while from those of order $O(\varepsilon)$ we find

$$-\nu h_2 = h_1 \frac{\partial h_0}{\partial y_1} + h_0 \frac{\partial h_1}{\partial y_1} + y_1 \frac{\partial h_1}{\partial y_2}.$$

Then, it results

$$h_1 = -\frac{1}{\nu} \left\{ -\frac{1}{\nu} h_0 F_\eta'(y_1) - \frac{\tilde{c}}{\nu} y_1 \right\} = \frac{1}{\nu^2} F_\eta'(y_1) \left[F_\eta(y_1) + \tilde{c} y_2 \right] + \frac{\tilde{c}}{\nu^2} y_1,$$

and as a consequence

$$\begin{aligned} \frac{\partial}{\partial y_1} h_1 &= \frac{1}{\nu^2} F_\eta''(y_1) \left[F_\eta(y_1) + \tilde{c} y_2 \right] + \frac{1}{\nu^2} \left[F_\eta'(y_1) \right]^2 + \frac{\tilde{c}}{\nu^2}, \\ \frac{\partial}{\partial y_2} h_1 &= \frac{\tilde{c}}{\nu^2} F_\eta''(y_1). \end{aligned}$$

Finally, the second order term is

$$h_2(y_1,y_2) = \frac{1}{\nu^4}[F'_\eta(y_1)]^2[F_\eta(y_1)+\tilde{c}y_2] + \frac{\tilde{c}}{\nu^4}y_1F'_\eta(y_1) + \frac{\tilde{c}^2}{\nu^4}y_1y_2 + \frac{\tilde{c}}{\nu^4}y_1F_\eta(y_1)$$
$$+\frac{1}{\nu^3}F''_\eta(y_1)\left\{-\tilde{c}y_1 + \frac{\tilde{c}^2}{\nu}y_2^2 + \frac{1}{\nu}F_\eta(y_1)[F\eta(y_1)+2\tilde{c}y_2]\right\}.$$

From Fenichel's Theorem (Theorem 11.1.1, page 328 in [13]) the dynamics on the slow manifold S_ε is given by

$$\begin{cases} \dot{y_1} = g_1(h_\varepsilon(y_1,y_2),y_1,y_2) = h_\varepsilon(y_1,y_2), \\ \dot{y_2} = g_2(h_\varepsilon(y_1,y_2),y_1,y_2) = y_1. \end{cases} \tag{3.10}$$

We note that at order $O(1)$ we find again Van Der Pol equation.
In figure 4 below we represent the numerical solution of system (3.1) computed with the software Mathematica and the approximated slow Manifold. We observe that the approximation of the slow manifold is good as the periodic orbit lies on it with a good adherence.

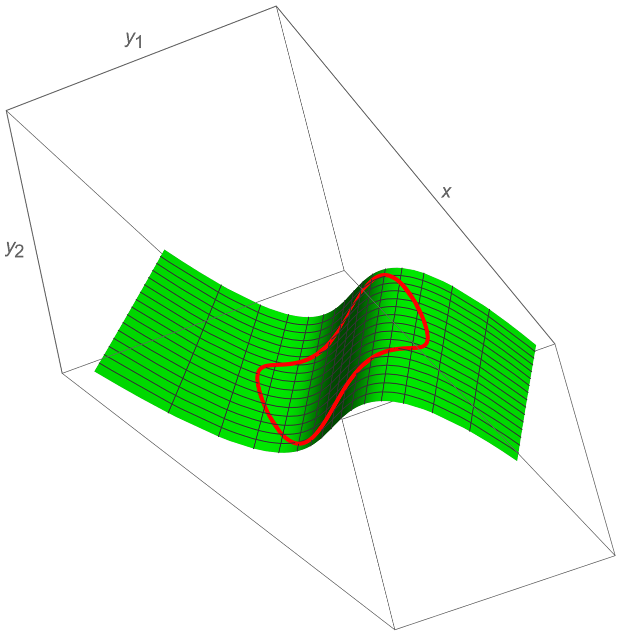

FIGURE 4. The numerical solution (in red) of system (3.2) on the approximated slow manifolds $x = \tilde{h}_\varepsilon(y_1,y_2) := h_0(y_1,y_2)+\varepsilon h_1(y_1,y_2)+\varepsilon^2 h_2(y_1,y_2)$ with $\varepsilon = 0.1, \nu = 1, \tilde{c} = 1$.

The above periodic orbit gives rise to a periodic travelling waves for the evolution equation (1.1). The problem of the stability ([11], [10]) of the wave trains is interesting and in general very difficult and several different approaches are used by researchers such as orbital [1], spectral and modulation stability ([12]). The stability analysis can be considered a natural continuation of the present research.

4. A different proof of limit cycle existence for WDP equation

In this section we provide a new (up to our knowledge) prove of the existence of a limit cycle for the Van der Pol equation.
For simplicity we rewrite the Van der Pol equation in the following way:

$$\begin{cases} \dot{x} = y, \\ \dot{y} = k[g(y) - x], \end{cases} \tag{4.1}$$

where

$$k := \frac{\tilde{c}}{\nu} > 0, \qquad g(y) := -\frac{1}{\tilde{c}} y(\eta y^2 - 1).$$

4.1. Construction of the positive invariant region

We define the following two variable function

$$G(x, y) = g(y) - x,$$

and consider its level curves

$$G(x, y) = \rho, \qquad \rho \in \mathbb{R}.$$

We introduce the following parametrization

$$\gamma_\rho(y) = (g(y) - \rho, y),$$

whose tangent vector is given by

$$\gamma'_\rho(y) = (g'(y), 1).$$

We observe that the zero level curve $\gamma_0(y)$ represents the $y-$isocline of system (4.1).
We consider the curve $\gamma_{-\rho}$ with $\rho > 0$ and choose the orientation such that the tangent vector is given by

$$\gamma'_{-\rho}(y) = (-g'(y), -1) := T = (T_x, T_y).$$

We limit to the case

$$y > \frac{1}{\sqrt{3\eta}},$$

from which it results that $T_x > 0$, $T_y < 0$.
On $\gamma_{-\rho}(y)$ the vector field of system (4.1) is

$$V = (y, -k\rho) := (V_x, V_y),$$

with $V_x > 0, V_y < 0$. We want to determine the portion, $\Gamma^+_{-\rho}$, of the curve $\gamma_{-\rho}$ such that the vector field points inward the region

$$\left\{ x, y \in \mathbb{R}^2 : \quad g(y) + \rho < x, \quad \text{with} \quad y > \frac{1}{\sqrt{3\eta}} \right\}.$$

Due to the sign of the components of V and T it is sufficient to impose

$$\frac{k\rho}{y} > -\frac{1}{g'(y)},$$

which produces

$$3\eta y^2 - \frac{\nu}{\rho} y - 1 > 0.$$

Since we require $y > 0$ we obtain

$$y > y_+ := q + \sqrt{q + \frac{1}{3\eta}},$$

where $q := \frac{\nu}{6\eta\rho} > 0$. We observe that $y_+ > \frac{1}{\sqrt{3\eta}}$ and that for $y = y_+$ the two vectors T and V are parallel.
Then the set $\Gamma^+_{-\rho}$ is defined as the portion of the curve $\gamma_{-\rho}$ with $y \geq y^+$, moreover, we define $x_+ := g(y_+) + \rho$ and $P^+ := (x_+, y_+)$.
We observe that if the initial datum (x_0, y_0) satisfies $x_0 \leq x_+$, $y_0 \geq y_+$ and (x_0, y_0) is below the curve $\Gamma^+_{-\rho}$ then the corresponding solution of system (4.1) can not cross $\Gamma^+_{-\rho}$ except at the point P^+.
Before to proceed we observe that $y_+ > 0$ and that

$$\lim_{\rho\to 0^+} y_+ = +\infty, \qquad \lim_{\rho\to +\infty} y_+ = \frac{1}{\sqrt{3\eta}},$$

moreover $\frac{\partial}{\partial\rho} y_+ < 0$ and as a consequence y_+ is strictly decreasing with respect to ρ. It is easy to see that $\frac{\partial^2}{\partial\rho^2} y_+ > 0$. Regarding x_+ we have that

$$\lim_{\rho\to 0^+} x_+ = -\infty, \qquad \lim_{\rho\to +\infty} x_+ = +\infty,$$

and

$$\frac{\partial}{\partial\rho} x_+ = g'(y_+) \frac{\partial}{\partial\rho} y_+ + 1 > 0,$$

since $y_+ > \frac{1}{\sqrt{3\eta}}$ and in this interval of values $g'(y)$ is negative. Then x_+ is strictly increasing and as a consequence there exists a unique $\rho^* \in (0, +\infty)$ such that $x_+(\rho^*) = 0$. Moreover it is easy to see that $\frac{\partial^2}{\partial\rho^2} x_+ < 0$.
Now we consider the straight line r^+ trough P^+ with direction $(y_+, k[g(y_+) - x_+]) = (y_+, -k\rho)$:

$$r^+ : \quad \begin{cases} x = x_+ + t y_+, \\ y = y_+ - t k \rho. \end{cases}$$

The above line is tangent to the curve $\gamma_{-\rho}$ at P^+ and since the curve is convex, the line is always above it. Let $m_\rho = -\frac{k\rho}{y_+} < 0$ be its slope, then

$$\frac{\partial}{\partial\rho} m_\rho = -k \frac{y_+ - \rho y_+'}{y_+^2} < 0,$$

since

$$y_+ - \rho y_+' = y_+ - \rho \frac{\partial q}{\partial\rho} \left(1 + \frac{1}{2\sqrt{q + \frac{1}{\sqrt{3\eta}}}} \right) > 0,$$

where we have used that $\frac{\partial q}{\partial \rho} < 0$.
The line r^+ intersects the $x-$axis at the point

$$F^+ := (F_x^+, F_y^+) := \left(x_+ + \frac{y_+^2}{k\rho}, 0 \right),$$

with

$$\lim_{\rho \to 0^+} F_x^+ = \lim_{q \to +\infty} 5 \frac{\eta}{\tilde{c}} q^3 = +\infty, \qquad \lim_{\rho \to +\infty} F_x^+ = \lim_{\rho \to +\infty} x_+ = +\infty.$$

Then there exists at least one minimum. Then we can always find an interval of the form $(0, \rho_1)$, (ρ_k, ρ_{k+1}), or $(\rho_n, +\infty)$ in which the segments P^+F^+ do not intersect between them.

Theorem 4.1. *For any $\rho > 0$, the region R_ρ delimited by the curve $\Gamma_{\pm\rho}$ and the segments P^+F^+, F^+A^-, P^-F^-, F^-A^+ (see figure 5) is positively invariant.*

Proof. Thanks to the above construction we have that on the segment P^+F^+ it results $\dot{y} < 0$ and as a consequence $\dot{x} = y$ is decreasing. For this reason on P^+F^+ the vector field V points inward the region below the segment P^+F^+ with $x_+ \le x \le F_x^+$. Then, if the initial datum (x_0, y_0) is below the segment P^+F^+ with $y_+ > y_0 > 0$ and $F_+ \ge x_0 \ge x_+$, the corresponding solution can not cross the segment P^+F^+ except at F^+ at which the vector field V is vertical.
We consider the intersection of the vertical line through F^+ and the curve γ_ρ and denote the intersection point as A^-. We observe that on the segment F^+A^- the vector field V points to the left and as a consequence solutions can not cross it from the left.
Using the symmetry of the problem we construct the curve Γ_ρ and the points P^-, F^- and A^+ as the symmetric with respect the origin of the points P^+, F^+ and A^+ respectively and this completes the proof. □

The dynamics inside R_ρ is completely determined by the following result.

Theorem 4.2. *Let $\rho > 0$. There exists a closed orbit inside the region R_ρ toward which solutions starting in R_ρ converge.*

Proof. The positively invariant region R_ρ contains only one equilibrium, that is $O = (0, 0)$, which is repelling. We observe that there are no homoclinic orbits to O since the unstable manifold of O is bidimensional. From Poincaré-Bendixon theorem we conclude that there exists a periodic orbit toward which solutions starting inside R_ρ converge. □

The following result describe some properties of the periodic orbits.

Theorem 4.3. *The Periodic orbits of system* (4.1) *are symmetric with respect the origin O and are outside the rectangle $\mathcal{R}$ (see* (4.2)*).*

Proof. From Bendixon-Dulac Theorem we have that there are no periodic orbits entirely contained in regions where the divergence of the vector field has constant sign:

$$\operatorname{div}(V) = kg'(y) = -\frac{1}{\nu}(3\eta y^2 - 1).$$

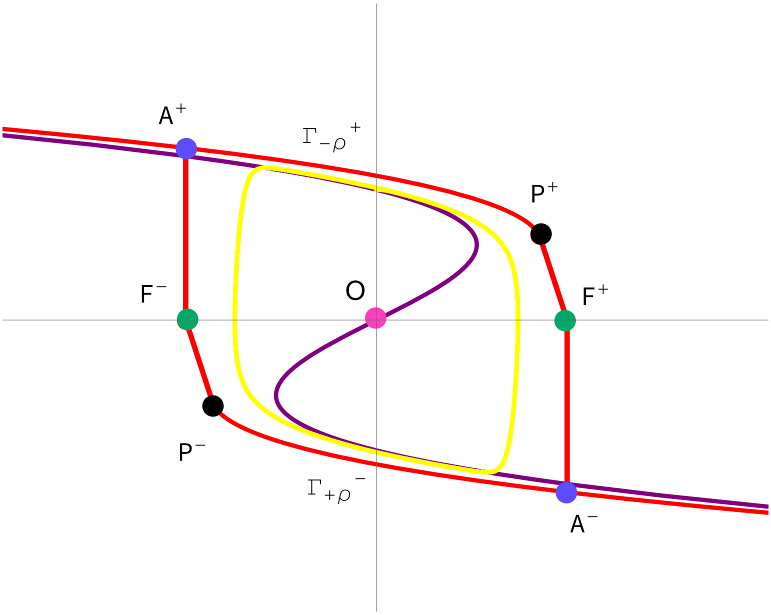

FIGURE 5. The positively invariant region (in red) R_ρ, the y-isocline (in violet) and the numerical solution of (4.1) with $\eta = 1, \tilde{c} = 1, \nu = 1$ and $\rho = 2$.

Then there are no periodic orbits entirely contained in the following regions:

$$B^+ := \left\{ (x, y) \in \mathbb{R}^2 : \quad y > \frac{1}{\sqrt{\eta}} \right\};$$

$$B^- := \left\{ (x, y) \in \mathbb{R}^2 : \quad y < -\frac{1}{\sqrt{\eta}} \right\};$$

$$C := \left\{ (x, y) \in \mathbb{R}^2 : \quad -\frac{1}{\sqrt{\eta}} < y < \frac{1}{\sqrt{\eta}} \right\}.$$

Moreover, since $\dot{x} = y$, periodic orbits are not completely contained in the semi-plane $y > 0$ or in $y < 0$, and as a consequence they intersect the $x-$axis. Since the $y-$isocline is given by $g(y) - x = 0$ periodic orbits can not remain completely in the region $g(y) - x > 0$ or in $g(y) - x < 0$ that is to the left or to the right of γ_0.

From the above argument we conclude that a periodic orbit must intersects the $x-$axis and the curve γ_0 at least in two points. We denote by $X_1 := (x_1, 0)$ and $X_2 := (x_2, 0)$ with $x_1 > 0 > x_2$ the intersections with the x-axis while by $G_1 := (g_1^x, g_1^y)$ and $G_2 := (g_2^x, g_2^y)$ with $g_1^y > 0 > g_2^y$ the intersections with the curve γ_0.

We suppose that a periodic orbit has a third intersection $x_3 > 0$ with the $x-$axis, then:

if $0 < x_3 < x_1$ the set whose boundary consists of the orbit from x_1 to x_3 and the segment from x_1 to x_3 is positively invariant and as a consequence, since self intersections are not permitted, the orbit can not pass again trough the point x_1;
if $0 < x_1 < x_3$ the orbit can not cross the curve made up of the portion of the periodic orbit from x_1 to x_3 and of the segment $x_1 x_3$ and as a consequence it can not reach again the point x_1. From the above argument we obtain that a periodic orbit has only two intersections $x_1 > 0 > x_2$ with the x-axis.
By a same reasoning we obtain that a periodic orbit has only two intersections with the curve γ_0.
We observe that from G_1 to X_1 the periodic orbit $(x(t), y(t))$ is monotone in the sense that $x(t)$ is increasing and $y(t)$ is decreasing and as a consequence the $y-$component of G_1 is its maximum value, similar monotonic properties are valid in the other portions of the orbit.
From the above analysis and from the expression of the vector field we conclude that

$$G_1^y \geq \frac{1}{\sqrt{3\eta}}, \quad G_2^y \leq -\frac{1}{\sqrt{3\eta}}, \quad x_1 \geq \gamma_0(G_1^y), \quad x_2 \leq -\gamma_0(G_1^y).$$

Then the periodic orbit is outside the rectangle (see figure 6)

$$\mathcal{R} := \left[-\frac{1}{\sqrt{3\eta}}, \frac{1}{\sqrt{3\eta}}\right] \times \left[-\frac{2}{3\tilde{c}\sqrt{3\eta}}, \frac{2}{3\tilde{c}\sqrt{3\eta}}\right], \tag{4.2}$$

and for the above reasoning, is a closed loop around the origin.
From the equations of the system we obtain that if $(x(t), y(t))$ is a solution also $(-x(t), -y(t))$ is a solution. Suppose that then periodic orbit starting at $(x_2, 0)$ intersects the $x-$axis at $(x_1, 0)$ with $|x_2| > x_1$, by symmetry there exists a periodic orbit starting at $(-x_2, 0)$ intersecting the $x-$axis at $(-x_1, 0)$ Then the two portions of the orbit together with the horizontal segments cannot be crossed by solutions contradicting the fact that periodic solutions have only two intersections with the x-axis. We conclude that $x_1 = -x_2$ and with the same reasoning we obtain $G_1 = -G_2$.
We call the portion of the periodic orbit from x_2 to x_1 $\sigma(t)$, from the above reasoning there exists a solution $-\sigma(t)$ from $-x_2$ to $-x_1$, but since $-x_2 = x_1$, by uniqueness of solutions we obtain that $-\sigma(t)$ is a portion of the same periodic orbit. That is the periodic orbit is symmetric with respect the origin.
□

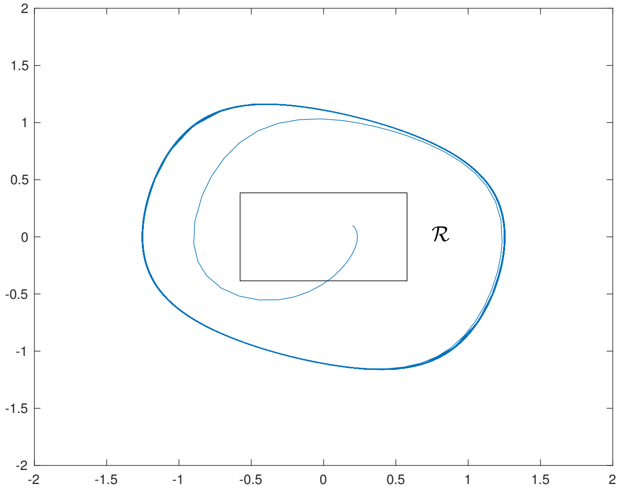

FIGURE 6. The rectangle $\mathcal{R}$. Initial data are chosen inside $\mathcal{R}$, the solution leaves the rectangle as the limit cycle surround it.

5. Stationary Solutions

In this section we study the set of stationary solutions of equation (1.1), that is, solutions of the following ODE:

$$\varepsilon u_{xxxx} + \nu u_{xxx} + [W'_\eta(u_x)]_x = 0. \tag{5.1}$$

By integration we obtain a third order ODE

$$\varepsilon u_{xxx} + \nu u_{xx} + [W'_\eta(u_x)] = K, \tag{5.2}$$

where for simplicity we set $K = 0$.
In order to study the qualitative properties of the solutions of the previous equation we introduce the following energy function:

$$H(u) := \frac{1}{2}\varepsilon u_{xx}^2 + W_\eta(u_x),$$

whose derivative along the solution of (5.2) is

$$\frac{d}{dx}H(u) = -\nu u_{xx}^2.$$

Thus, H is decreasing and since it is bounded from below it converges for $x \to +\infty$ to a non negative number $a \geq 0$.
If we set $u_x = v$ we obtain the following second order ODE

$$\varepsilon v_{xx} + \nu v_x + W'_\eta(v) = 0, \tag{5.3}$$

that we rewrite as a system of two first order ODE's:

$$\begin{cases} \dot{v} = w, \\ \varepsilon \dot{w} = -\nu w - W'_\eta(v). \end{cases} \tag{5.4}$$

The above system has three fixed points: $O_{vw} = (0,0)$ and $P^\pm = \left(\pm\frac{1}{\sqrt{\mu}}, 0\right)$.
The Jacobian matrix of (5.4) is:

$$J = \begin{pmatrix} 0 & 1 \\ \frac{1}{\varepsilon}(1 - 3\eta v^2) & -\frac{\nu}{\varepsilon} \end{pmatrix},$$

from which

$$J_{O_{vw}} = \begin{pmatrix} 0 & 1 \\ \frac{1}{\varepsilon} & -\frac{\nu}{\varepsilon} \end{pmatrix}, \qquad J_{P^\pm} = \begin{pmatrix} 0 & 1 \\ -\frac{2}{\varepsilon} & -\frac{\nu}{\varepsilon} \end{pmatrix}.$$

The point O is a saddle since the eigenvalues of J_O are $\lambda_{1,2} = \frac{-\nu \pm \sqrt{\nu^2 + 4\varepsilon}}{2\varepsilon}$ and have opposite sign. The eigenvalues of $J_{P^\pm}$ are $\lambda_{1,2} = \frac{-\nu \pm \sqrt{\nu^2 - 8\varepsilon}}{2\varepsilon}$. If $\nu \in (0, 2\sqrt{2\varepsilon})$ then $P^\pm$ are stable foci, while for $\nu \geq 2\sqrt{2\varepsilon}$ they are stable nodes.

Theorem 5.1. *All solutions of system* (5.4) *converge to one of the fixed points.*

Proof. We first observe that for the vector field $F = (w, -\frac{\nu}{\varepsilon}w - \frac{1}{\varepsilon}W'_\eta(v))$ we have

$$divF = -\frac{\nu}{\varepsilon} < 0,$$

then from Bendixon-Dulac Theorem we exclude the existence of periodic orbits.

By monotonicity of the function H we exclude the existence of homoclinic orbits for the three fixed points. Moreover

$$H(O_{vw}) = \frac{1}{4\eta}, \qquad H(P^{\pm}) = 0,$$

and using the stability analysis we obtain the existence of only two heteroclinic connections that connect O_{vw} to P^+ and P^- respectively (the unstable curves). We note that the stable curves of O_{vw} separate the basin of attraction of the two stable fixed points $P^{\pm}$. Using La Salle Principle and the above analysis we conclude that any solution of (5.4) converges to P^+ or P^- except the stable manifolds of O_{vw}.

□

Remark 5.2. *From the previous theorem, we note that solutions of system* (5.4) *satisfy*

$$\lim_{\xi \to +\infty} H(x) = 0,$$

except the stable curves of O_{vw} *for which*

$$\lim_{\xi \to +\infty} H(x) = \frac{1}{4\eta}.$$

Coming back to the solutions of the complete system we obtain:

Theorem 5.3. *The stationary solutions of equation* (1.1) *can be classified into three groups:*

(A) *solutions converging to* $u^+(x) = \frac{1}{\sqrt{\eta}}x + c$ *as* $x \to +\infty$*;*

(B) *solutions converging to* $u^-(x) = -\frac{1}{\sqrt{\eta}}x + c$ *as* $x \to +\infty$*;*

(C) *solutions converging to a constant solutions* $u_c \equiv c$ *as* $x \to +\infty$*;*

where c is a real constant.

Proof. We first observe that the three dimensional system has a line of fixed points of the form $(l, 0, 0)$ corresponding to constant solutions of the evolution equation. If $(v_x(0), v_{xx}(0)) \in W_s(O)$ then solutions of (5.1) converge to a constant solution of this family. If the initial data, are such that in the (v_x, v_{xx}) plane they belong to the basin of attraction of P^+, or to its right stable curve, then the corresponding solutions of (1.1) converges to a function of the family of $u^+(x)$. An analogous result is valid for $u^-(x)$. □

In figures 7, 8 below we represent two solutions converging to $u^-(x)$ and $u^+(x)$ respectively.

6. Conclusion

In this article we have studied the travelling wave and stationary solutions of a nonlinear fourth order evolution equation. For certain values of the parameters we have excluded the existence of travelling waves while in other cases we have proved the existence of periodic travelling waves. The existence of

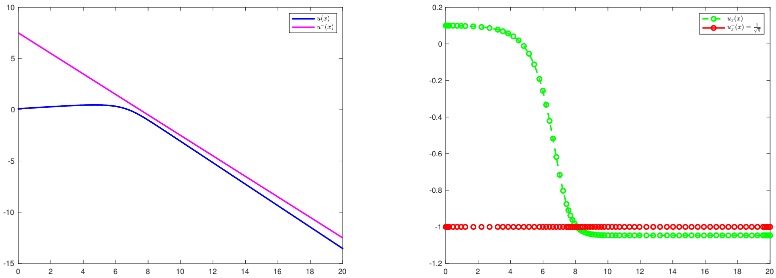

FIGURE 7. The numerical solution of (5.2) converging to $u^{-}(x)$ as $x \to +\infty$ and their derivatives.

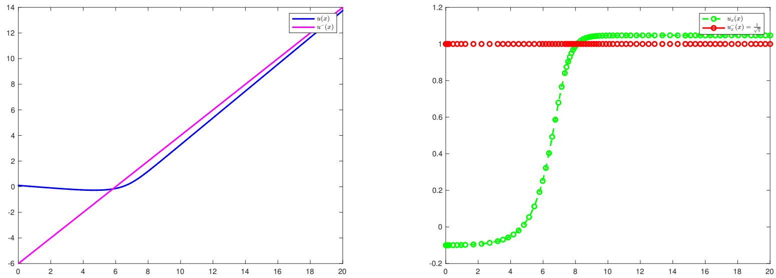

FIGURE 8. The numerical solution of (5.2) converging to $u^{+}(x)$ as x$\to +\infty$ and their derivatives.

solitary waves and the stability of periodic travelling waves are left for further research.

References

[1] Alves G., Natali F., Pastor A. Sufficient conditions for orbital stability of periodic travelling waves (2019) Journal of Differential Equations, 267 (2), pp. 879 - 901.

[2] Bennett J.J.R., Sherratt J.A. Periodic traveling waves generated by invasion in cyclic predator-prey systems: The effect of unequal dispersal (2017) SIAM Journal on Applied Mathematics, 77 (6), pp. 2136 - 2155.

[3] Bennett J.J.R., Sherratt J.A. How do dispersal rates affect the transition from periodic to irregular spatio-temporal oscillations in invasive predator–prey systems? (2019) Applied Mathematics Letters, 94, pp. 80 - 86.

[4] Chen H., Bona J.L. Periodic traveling-wave solutions of nonlinear dispersive evolution equations (2013) Discrete and Continuous Dynamical Systems- Series A, 33 (11-12), pp. 4841 - 4873.

[5] Claassen K.M., Johnson M.A. Numerical Bifurcation and Spectral Stability of Wavetrains in Bidirectional Whitham Models (2018) Studies in Applied Mathematics, 141 (2), pp. 205 - 246.

[6] R. Colucci, Special solutions for an equation arising in sand ripple dynamics, *Nonlinear Analysis: Real World Applications*, Volume 67, 2022.

[7] F. Verhulst *Methods and Applications of Singular Perturbations*, Springer, 2005.

[8] Friedrichs K.O.,Wasow W.R. *Singular perturbations of non-linear oscillations* , Duke mathematical journal,13(3), 1946, p. 367-381.

[9] M. W. Hirsch, S. Smale, R. L. Devaney, *Differential Equations, Dynamical Systems, and an Introduction to Chaos* (Third Edition), Academic Press, 2013.

[10] Hakkaev S., Stanislavova M., Stefanov A. On the Stability of Periodic Waves for the Cubic Derivative NLS and the Quintic NLS (2021) Journal of Nonlinear Science, 31 (3), art. no. 54.

[11] Jones C.K.R.T., Marangell R., Miller P.D., Plaza R.G. On the stability analysis of periodic sine-Gordon travelling waves (2013) Physica D: Nonlinear Phenomena, 251, pp. 63 - 74.

[12] Jones C.K.R.T., Marangell R., Miller P.D., Plaza R.G. Spectral and modulational stability of periodic wave trains for the nonlinear Klein-Gordon equation (2014) Journal of Differential Equations, 257 (12), pp. 4632 - 4703.

[13] C. Kuehn, *Multiple Time Scale Dynamics*, Springer International Publishing, Switzerland 2015.

[14] Zhang G. New periodic exact travelling wave solutions of Camassa–Holm equation (2022) Partial Differential Equations in Applied Mathematics, 6, art. no. 100426.

[15] Deng D., Wang J., Zhang L. Critical periodic travelling waves for a Kermack-McKendrick epidemic model with diffusion and seasonality (2022) Journal of Differential Equations, 322, pp. 365 - 395.

Renato Colucci
Dipartimento di Ingegneria
e Scienze Matematiche,
Università Politecnica delle Marche,
via delle Brecce Bianche 12,
60131 Ancona, Italy
e-mail: `r.colucci@univpm.it`